BMC Chemistry

RESEARCH ARTICLE

Open Access

Magnetic γFe_2O_3@Sh@Cu_2O: an efficient solid-phase catalyst for reducing agent and base-free click synthesis of 1,4-disubstituted-1,2,3-triazoles

Fereshteh Norouzi and Shahrzad Javanshir*

Abstract

A hybrid magnetic material γFe_2O_3@Sh@cu_2O was easily prepared from Shilajit (Sh) decorated Fe_3O_4 and copper acetate. The prepared magnetic hybrid material was fully characterized using different analysis, including Fourier transform infrared (FT-IR), X-ray diffraction (XRD), inductively coupled plasma (ICP), scanning electron microscopy (SEM), Energy-dispersive X-ray spectroscopy (EDX), X-ray photoelectron spectroscopy (XPS), vibrating sample magnetometer (VSM) thermal gravimetric analysis (TGA) and Brunauer–Emmett–Teller (BET). All these analysis revealed that during coating of Fe_3O_4@Sh using copper salt (II), synchronized redox sorption of Cu^{II} to Cu^{I} occurs at the same time as the oxidation of Fe_3O_4 to γFe_2O_3. This magnetic catalyst exhibited excellent catalytic activity for regioselective synthesis of 1,4-disubstituted-1,2,3-triazoles via one pot three-component click reaction of sodium azide, terminal alkynes and benzyl halides in the absence of any reducing agent. High yields, short reaction time, high turnover number and frequency (TON = $3.5 * 10^5$ and TOF = $1.0 * 10^6$ h^{-1} respectively), easy separation, and efficient recycling of the catalyst are the strengths of the present method.

Keywords: Click synthesis, Hybrid magnetic material, Heterogeneous catalyst, Shilajit, Humic acids

Introduction

Presented by Sharpless [1] in 2001, the "click chemistry" consists of clipping two molecules to one another, as one closes a snap. However, not all molecules can be clipped to any other. The reaction involves an alkyne and a nitrogen-based group. For the past ten years, click chemistry has been the subject of much research. The coupling between azides and alkynes is part of the so-called bioorthogonal chemical reactions, biocompatible reactions and a high selectivity. While click chemistry has everything to seduce the world of life, it has a weak point: its kinetics is extremely low, hence the frequent use of a catalyst, copper. The introduction of copper catalysis in 2001, independently by Meldal [2] and Sharpless groups [1] led to a major advance in both speed and regioselectivity of the reaction, where only 1,4-regioisomer is formed, and made it a reaction that respected the criteria of click chemistry.

According to the literature, several sources make it possible to obtain Cu^{I} ions in the reaction mixture. In situ reduction of copper(II) salts in the form of copper sulphate pentahydrate ($CuSO_4 \cdot 5H_2O$) or copper acetate ($Cu(OAc)_2$), is the most commonly encountered method. It requires the introduction of an excess reducing agent, usually sodium ascorbate. Oxidation of metallic copper is another way of generating copper(I). The reaction is done by adding a large excess of copper to the azide/alkyne mixture. Until now, the Huisgen's copper(I)-catalyzed

*Correspondence: Shjavan@iust.ac.ir
Heterocyclic Chemistry Research Laboratory, Department of Chemistry, Iran University of Science and Technology, Tehran 16846-13114, Iran

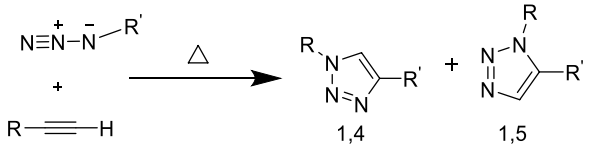

Fig. 1 1,3-Dipolar azide/alkyne cycloaddition from Huisgen

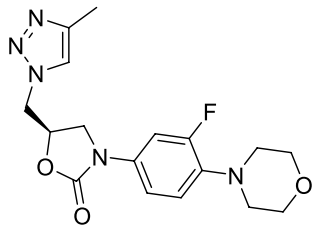

(1)

Fig. 2 (*S*)-3-(3-Fluoro-4-morpholinop henyl)-5-((4-methyl-1*H*-1,2,3-triazol-5-yl)methyl)oxazolidin-2-one

azide-alkyne cycloaddition (CuAAC) remain the most popular reaction making possible to rapidly, quantitatively, and reproducibly obtain a large variety of five-membered heterocycles via heteroatomic bonds [1–12]. However, the classical conditions of Huisgen reaction necessitates elevated temperatures, prolonged reaction times and lead to a mixture of isomeric 1,4- and 1,5-triazoles (Fig. 1).

From a biological point of view compounds comprising a triazolic group in their structures have largely aroused the attention of chemists as they present a wide range of rather potent biological activities. Demonstrating a high aromatic stability, it is resistant to acidic and basic hydrolysis, reducing and oxidative conditions and metabolic degradation. This heterocycle is therefore a good candidate for use as a modified nucleoside base [13]. Medicinal chemists have examined heterocycle synthesis based on 1,2,3-triazole as the cornerstone of medicinal chemistry and pharmaceuticals because of their important biological activities. Phillips et al. synthesized 5-(4-methyl-1,2,3-triazole)methyloxazolidinones **1** (Fig. 2) and characterized their antibacterial activity in vitro against Gram-positive and Gram-negative bacteria [14]. For example, these compounds behave as rigid binding units, so they can mimic the electronic properties of the amide bonds without the same susceptibility to hydrolytic cleavage. The 1,2,3-triazole rings have a higher dipole moment than the amide bonds, which gives them electrophilic and nucleophilic properties close to those of the peptide bonds [15].

The development of improved copper catalysts is uninterrupted. Recently, the synthesis of "click analogues" of the multivalent neoglycoconjugates was also reported using the CuAAc and organic-soluble copper catalysts [16]. Lately, Yamada et al. [17] designed an amphiphilic solid-phase self-assembled polymeric copper catalyst for click chemistry. Newly, click reaction was applied to biomolecule labeling by RIKEN institute and assembly of a biocompatible triazole-linked gene by one-pot click-DNA ligation [18]. All this research carried out by groups of researchers, elucidates not only the importance of the click reaction but also the importance of designing new catalysts that meet the demanding criteria of sustainable chemistry.

To overcome the difficulty of catalyst separation, some heterogeneous catalyst have been made such as copper(I)-modified SiO_2 [4], nano ferrite-glutathione-copper (nano-FGT-Cu) [5], amberlyst A-21-copper(1) [6], Cu nano particles supported on agarose [7], Cu(I) on waste oyster shell powder [8], copper nanoparticles on charcoal [9], copper nanoparticles on activated carbon [1], Cu(I) supported on alumina (Cu/Al_2O_3) [1], copper immobilized onto a triazole functionalized magnetic nanoparticle [19], cellulose supported cuprous iodide nano particles [20], polymer supported copper [21], magnetic copper starch nanocomposite [22], knitted N-heterocyclic carbene-copper complex [23, 24], copper(I)-phosphinite complex [25], Fe_3O_4 nanoparticle-supported Cu(II)-β-cyclodextrin complex [26], Cu@PyIm-SBA-15 [27], Ag-Al_2O_3@Fe_2O_3 [28], and hierarchical mesoporous organic polymer Cu-HMOP [29] for the synthesis of 1,2,3-triazoles. Despite these achievements some of these heterogeneous catalyst have significant limitations such as using reducing agent to reduce Cu(II) to Cu(I), lack of regioselectivity, by-product production, high temperature, long reaction time, and difficult conditions. So more efficient, eco-friendly, economically and simpler procedures for the synthesis of 1,2,3-triazoles are considered.

Catalysis is an essential tool of green chemistry as it enables the development of less polluting chemical processes, improvement media and opens synthetic pathway to desired products using stable resources [30]. Significant properties of catalysts are their ability to be recovered and their eco-friendly behavior. Also the majority of industrial catalysts remain heterogeneous because of the simplicity of the latter in terms of recovery and eliminating the necessity of the catalyst filtration or centrifugation after completion of the reaction [31]. Furthermore, replacement of safe organic solvent instead of hazardous organic solvent has always been a concern in green chemistry [32]. With these aspects of green chemistry in mind, we have designed and synthesized γFe_2O_3@Sh@Cu_2O, a new catalysts for CuAAC reaction. Sh (mumlai in Farsi and mineral pitch in English) is a pale-brown to

blackish-brown exudates obtained from layer of rocks in many mountain ranges [33–36] and it is a mixture of 85% humic acids and 15% non-humic compounds. The principle bioactive in Sh being Fulvic acid, a powerful organic electrolyte known to balance plant and animal life by increasing the electrical potential for cell restoration [36].

We wish to report herein the design and synthesis of a novel magnetic heterogeneous catalyst, γFe_2O_3@Sh@Cu_2O, which, in minute amounts of 0.025 mol% promoted the click 1,3-dipolar cycloaddition of sodium azide, terminal alkynes and benzyl halides along with a high TOF up to $1.0*10^6$ (Fig. 3). γFe_2O_3@Sh@Cu_2O showed good recyclability without loss of catalytic activity that could occur as a result of oxidation of the Cu(I) species, which is thermodynamically unstable, or copper leakage.

Results and discussion

Preparation of magnetic γFe_2O_3@Sh@Cu_2O catalyst

The catalysts was prepared by a three step process (Fig. 4). First, Fe_3O_4 NPs were synthesized by co-precipitation method. For this purpose, $FeCl_3{\cdot}6H_2O$ and $FeCl_2{\cdot}4H_2O$, in a 2:1 molar ratio, were dissolved in water under stirring in an inert atmosphere of nitrogen. The chemical precipitation was accomplished at 70 °C by adding a solution of ammonium (15 mL, 30 w/w). Then, the mixture of Fe_3O_4 and glutaraldehyde as a crosslinking agent, was sonicated in EtOH. The Sh was then added and crosslinked onto the surfaces of Fe_3O_4/GA NPs. Finally, $CuBr_2$ and Fe_3O_4@Sh were clipped and thereby the hybrid magnetic catalyst was obtained after 2 h at 60 °C.

Characterization of prepared catalysts was performed by X-ray diffraction (XRD), Fourier transform infrared (FT-IR), field-emission scanning electron microscopy (FESEM), vibrating sample magnetometer (VSM) and X-ray photoelectron spectroscopy (*XPS*). The x-ray diffraction pattern in the 2θ range (10 to 80°) of Sh (Fig. 5a) exhibited small diffuse peaks with a few sharp peaks, implying its non-crystalline nature. XRD patterns of the prepared Fe_3O_4-Sh and γ-Fe_2O_3@Sh@Cu_2O show that a simultaneous redox reaction has taken place, in which Cu(II) was converted to Cu(I) and Fe_3O_4 to γFe_2O_3 (Fig. 5c, d). The main diffraction peaks at 2θ = 30.1, 35.4, 43.0, 47.1, 53.4, 56.9, 62.5, 70.9, 74.9 in Fe_3O_4 and Fe_3O_4@Sh attributed to (2 2 0), (3 1 1), (4 0 0), (3 3 1), (4 4 2), (5 1 1), (4 4 0), (6 2 0), (6 2 2) crystal planes show that the Fe_3O_4 NPs were formed in accordance with the standard card No [01-087-2334] and the diffraction peaks at 2θ = 30.48, 33.78, 35.74, 43.69, 49.5, 54.23, 57.56, 62.73 show that the magnetite γFe_2O_3 NPs were formed [37] in accordance with the standard card No [01-087-2334]. As observed recycled γFe_2O_3@Sh@Cu_2O retains its crystalline properties (Fig. 5e).

The average diameter of γFe_2O_3@Sh@Cu_2O nanoparticle was estimated to be 25.1 nm according to the Debye–Scherrer equation ($D = k\lambda/\beta COS\theta$). The small angle XRD pattern of γFe_2O_3@sh@Cu_2O is shown in Fig. 6. A broad peak at 2Θ 0.766° was observed which is assigned to the presence of mesostructure.

XRD characterization of the recycled catalyst was also performed. The characteristic peaks of catalyst were still observed in recycled γFe_2O_3@Sh@Cu_2O (Fig. 7) but with a significant decrease in the peak intensities. These results indicated that the structure was preserved upon after 5 run recycling; however, some collapse of the structure may have occurred (Additional file 1).

The FT-IR spectra of Fe_3O_4, Sh, Fe_3O_4@Sh, γFe_2O_3@Sh@Cu_2O, and recycled γFe_2O_3@Sh@Cu_2O after five runs are depicted in Fig. 8. The FT-IR spectrum of Sh

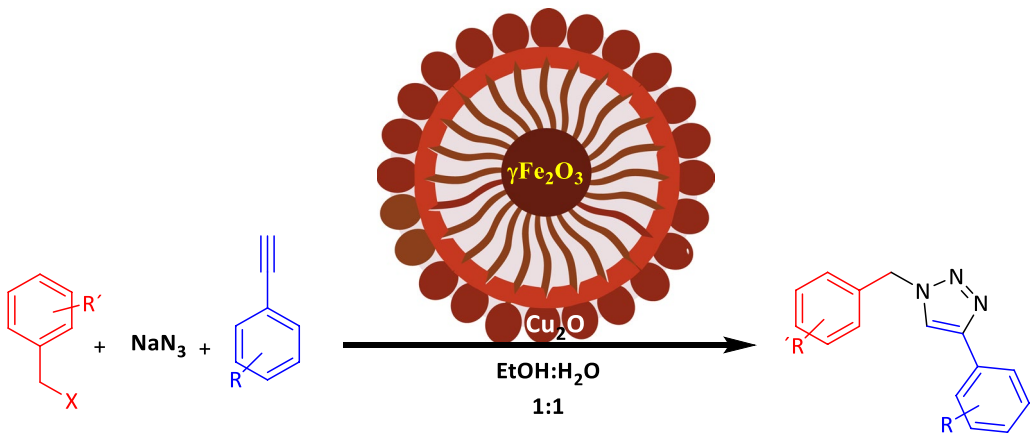

Fig. 3 One-pot synthesis of 1,2,3-triazoles catalyzed by γ-Fe_2O_3@Sh@Cu_2O

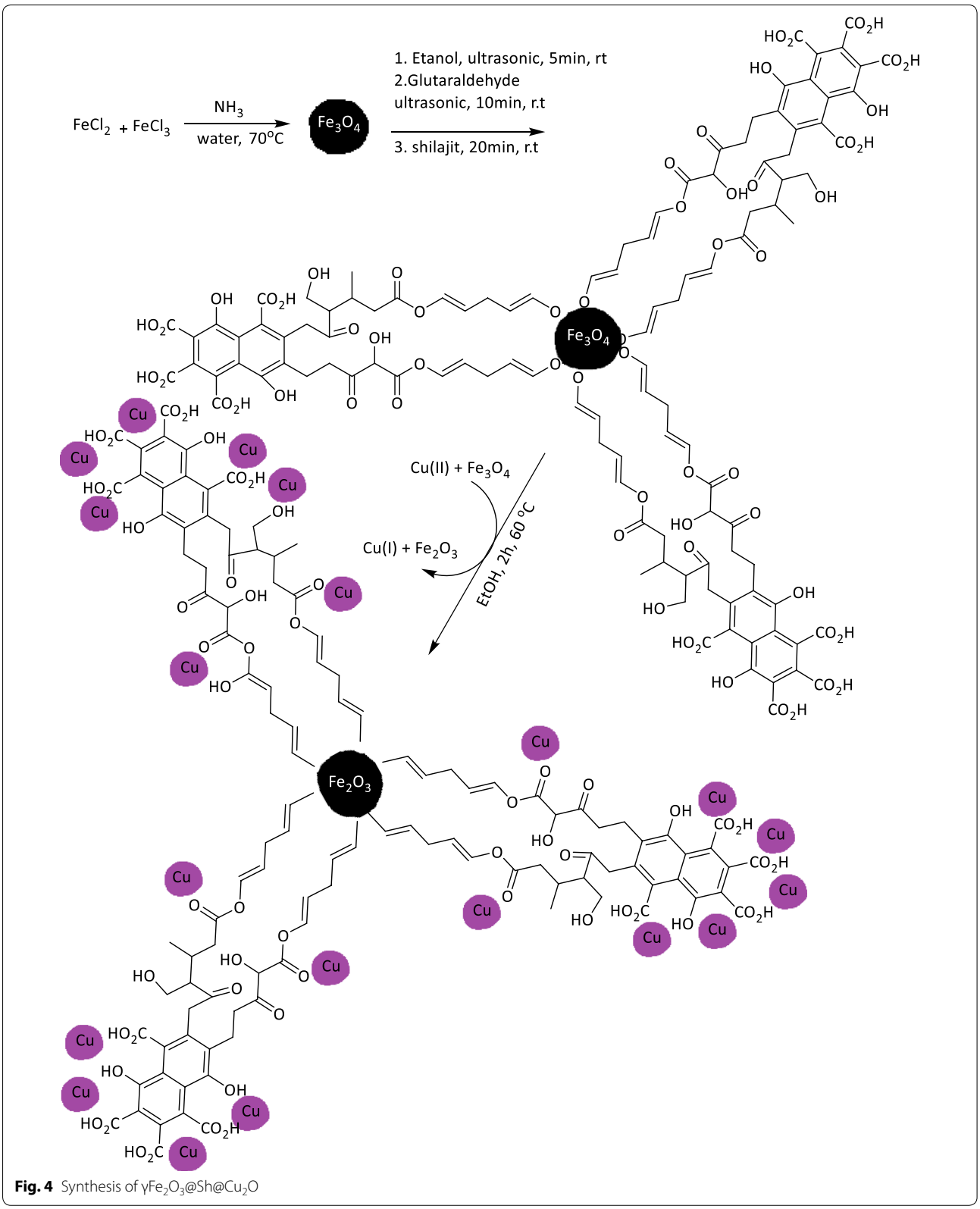

Fig. 4 Synthesis of γFe_2O_3@Sh@Cu_2O

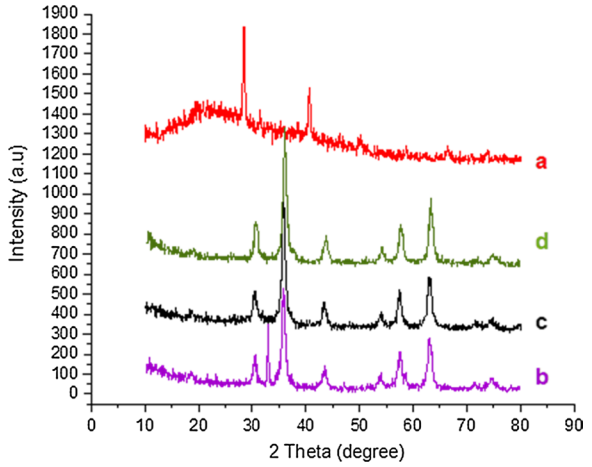

Fig. 5 XRD pattern of (a) Shilajit, (b) Fe_3O_4, (c) Fe_3O_4@Sh, (d) γFe_2O_3@Sh@Cu_2O

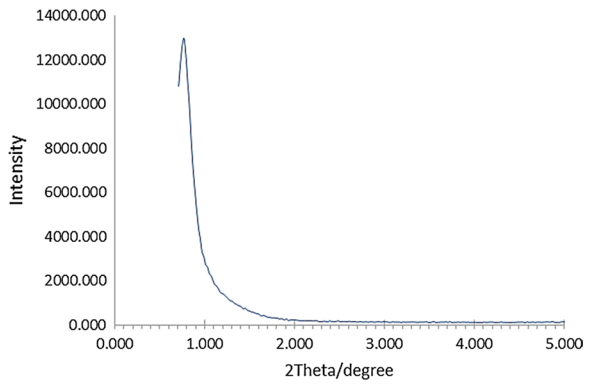

Fig. 6 Small angle XRD pattern of γFe_2O_3@Sh@Cu_2O

was characterized by few broad bands at 3400, 1700 and 1650 cm^{-1} which are attributed to hydrogen bonded OH group, the stretching vibration of the carbonyl group in COOH, and C=C double bonds. Sharp bands located in the region of 2925, 1400 and 1026 cm^{-1}, can be attributed to the bending vibration of aliphatic C–H groups, the O–H bending vibrations of alcohols or carboxylic acids and the OH bending deformation of carboxyl groups. For the IR spectrum of Fe_3O_4 the absorption band appeared at 580 cm^{-1} can be attributed to Fe–O [38]. As shown in Fig. 8, the absorption peaks in the infrared spectrum of γFe_2O_3@Sh@Cu_2O at low frequencies below 600 cm^{-1} are due to Cu–O vibration [39].

Also, the EDX of γFe_2O_3@Sh@Cu_2O discloses the presence of Fe, Cu, C and O in the structure of this material (Fig. 9). The copper content evaluated by ICP analysis was about 0.55%.

The XPS analysis of the γFe_2O_3@Sh@Cu_2O nanoparticles (Fig. 10) revealed the characteristics peaks for C 1s (284.88), O1s (530.39), Fe 2p (710.89) and Cu 2p (933.01). Moreover, the high resolution narrow scan for Fe 2p in γFe_2O_3@Sh@Cu_2O display energy peak of Fe2p3/2A and Fe2p1 at 710.8 and 724.3 eV respectively, which are characteristic peaks of the 3+ ion and clearly indicate the formation of the γ-Fe_2O_3 [40, 41]. Moreover, there exist satellite peak at 718.9 eV sides of the main doublet peaks, which also indicate the absence of the 2^+ ion, suggesting that the Fe_3O_4 nanoparticles were partly oxides and CuO nanoparticles were reduced, and γFe_2O_3@Sh@Cu_2O was created. The $Cu_2p3/2$ peaks located at 933.0 eV was attribute to Cu^1 in Cu_2O. Moreover, the O1s peaks at 530.4 eV are coherent with O-state in Cu_2O.

The morphology and size of Fe_3O_4, Fe_3O_4@Sh and the synthesized γFe_2O_3@Sh@Cu_2O NPs were investigated using SEM analysis (Fig. 11a–c). The SEM image of the synthesized γFe_2O_3@Sh@Cu_2O NPs (Fig. 11c) shows that morphology of the particles is spherical or quasi-spherical and the surface configuration of NPs is quite rough with smaller subunits. The average nanoparticle diameter of γFe_2O_3@Sh@Cu_2O was estimated 24–26 nm based on the SEM image.

The magnetic properties of the prepared γFe_2O_3@Sh@Cu_2O were measured by VSM at room temperature with the field sweeping from −8500 to +8500 oersted (Fig. 12). The magnetic curve of γFe_2O_3@Sh@Cu_2O revealed that it has super magnetic behavior, and its magnetization values was found to be 58 emu g^{-1}, so it could be efficiently separated by an external permanent magnet.

To investigate the thermal stability of catalyst, thermogravimetric analysis was carried out from 25 to 1000 °C under oxygen atmosphere condition. The TGA curves of Fe_3O_4, Fe_3O_4@Sh and γFe_2O_3@Sh@cu_2O, illustrating the variations of residual masses of the samples with temperature, are shown in Fig. 13a–c. The first mass loss of, 0.3% for Fe_3O_4 and γFe_2O_3@Sh@cu_2O and 0.6% for Fe_3O_4@Sh, observed below 260 °C, was attributed to moisture elimination. The total weight loss of the uncoated Fe_3O_4, Fe_3O_4@Sh and γFe_2O_3@Sh@cu_2O are 1.07, 3.1 and 1.7% respectively, which revealed that the thermal stability of γFe_2O_3@Sh was enhanced prominently after coating with Cu_2O.

The surface area and pore volume of γ-Fe_2O_3@Sh@Cu_2O were estimated from the N_2 adsorption/desorption isotherms and T-plot (Fig. 14a, b). Vertical plots from the straight line in T-plot indicated the presence of mesopores [42]. Applying the Barrett-Joyner-Halenda (BJH) method, indicates that the sample contains mesopores with diameters close to 23.655 nm and a surface area of 49.746 m^2/g.

Considering the efficiency of γFe_2O_3@Sh@Cu_2O, the reaction of benzyl chloride, sodium azide and phenyl

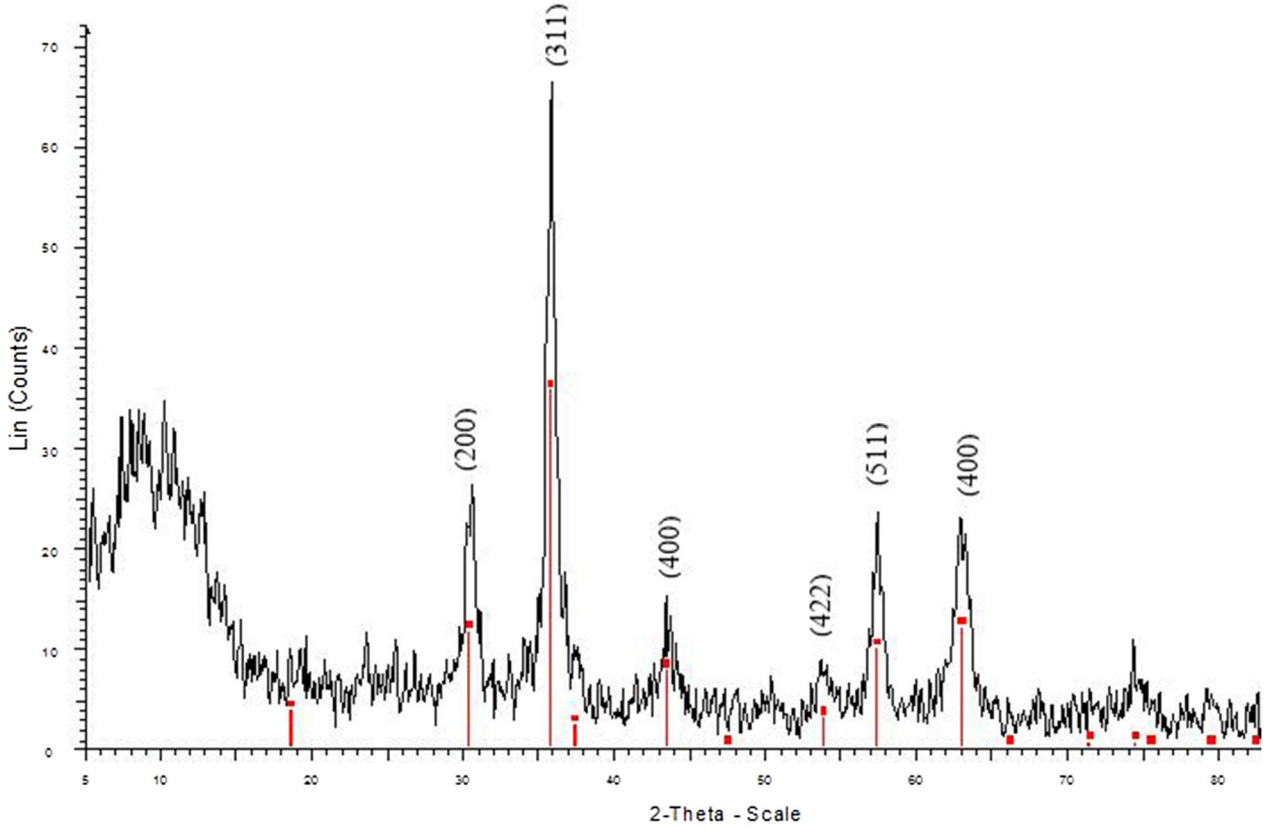

Fig. 7 XRD pattern of recycled γFe_2O_3@Sh@Cu_2O

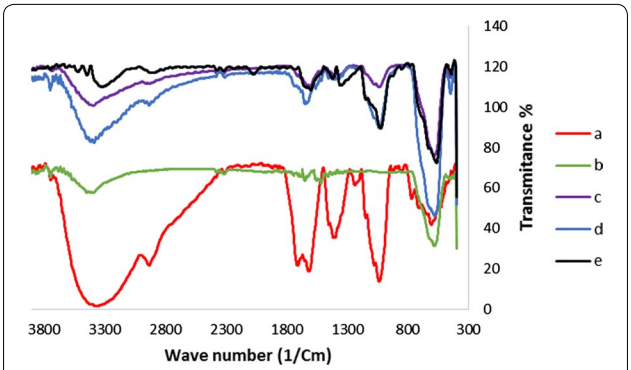

Fig. 8 FT-IR absorption spectra for (a) Shilajit, (b) Fe_3O_4, (c) Fe_3O_4@Sh, (d) γFe_2O_3@Sh@Cu_2O, (e) recycled γFe_2O_3@Sh@Cu_2O after 5 times use

acetylene approved as a model reaction. The impact of different parameters such as kinds and amounts of catalysts, solvents, time, and temperature reaction was checked to obtain the best combination condition. When the reaction was attempted without a catalyst in water, without water, at room temperature, at 80 °C that product was not obtained even after 48 h (Table 1, entry 1–4). To optimize the reaction conditions, several green solvents were used in different proportions. The effect of different solvents on the reaction efficiency is summarized in the Table 1. From Table 1, it was found that H_2O:EtOH (1:1) was the most effective solvent, while the use of other solvents such as EtOH and other proportions of H_2O:EtOH resulted in lower yields.

The reaction was carried out at different temperatures also (Table 1, entry 10–13), ranging from r.t to 100 °C and it was found that at 60 °C the yield of reaction was better than other temperatures and the reaction time was reduced to 45 min.

The influence of amount of catalyst on the yield and time was also investigated (Table 1, entry 14–18). By increasing the amount of catalyst from 5 to 40 mg, reaction efficiency increased by 93% and reaction time was decreased to 20 min. Further increase in catalyst amount had no profound effect on the yield of the desired product. Based on the above results, the optimal conditions were established to be the use of 30 mg γFe_2O_3@Sh@Cu_2O as the catalyst in H_2O:EtOH (1:1) at 60 °C. Some nano materials such as nano Fe_3O_4, $CuFe_2O_4$ with sodium ascorbate, Humic acid (HA), Fe_3O_4@HA, Fe_3O_4@HA@Cu, Sh, Fe_3O_4@Sh and some

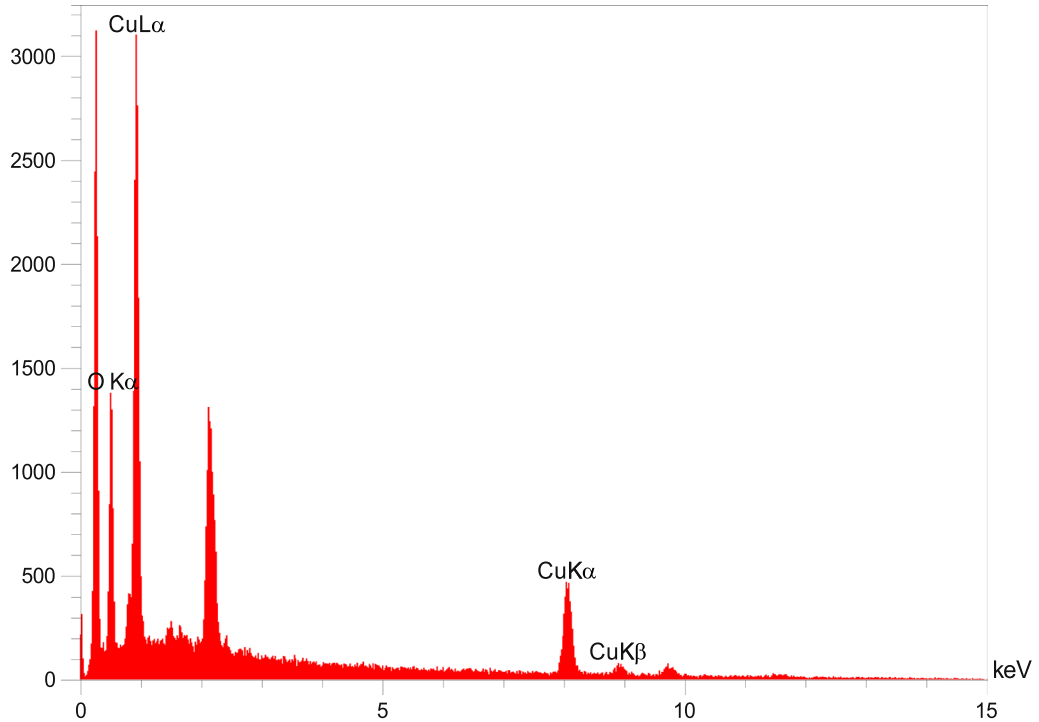

Fig. 9 EDX spectrum of γFe_2O_3@Sh@Cu_2O

copper salt such as $CuBr_2$ were test in optimum condition. However, in most cases, the reaction efficiency was not improved. A clear improvement of the yield was observed when Fe_3O_4@HA@Cu was added, which was foreseeable because it was the substance of the Sh, however the time is still longer than satisfactory (Table 2, entry 7).

In practice the effortlessness separation and recyclability are crucial factors for a heterogeneous catalyst. To evaluate the effectiveness of γFe_2O_3@Sh@Cu_2O, its recyclability was verified in the model reaction. After completion of the reaction, the catalyst was recovered by an external magnet and washed several times with EtOH, and then re-used after drying it at 60 °C. The recycled catalyst was used 5 times more, with little change in the efficiency and reaction time (Fig. 15).

The catalyst leaching study was performed to determine the heterogeneity of the solid catalyst. The catalytically active particles were removed from the reaction by filtration after 10 min using a hot frit. A reaction monitoring and metals measurement in solution indicated that there is practically no copper leaching during the reaction and the reaction rate decreased significantly after hot filtration (Fig. 16).

We began to make derivatives of this three-component reaction with the optimal reaction conditions we have in place. Different benzyl halides were explored under optimal conditions and the corresponding triazoles were obtained in good to excellent yields (Table 3). The reaction of terminal aryl alkyne bearing electron-donating or electron-withdrawing groups with benzyl halides and sodium azide leads to the corresponding products with high regioselectivity and yields. Satisfactorily, aryl alkyne having electron-donating substituents worked well and delivered expected products in high to excellent yields.

Next, the reactivity of various benzyl halides were evaluated. It has been observed that reaction does not occur well when we use benzyl halides with electron-withdrawing substituents. Therefore, it is predicted that the first part of the reaction, which is the formation of benzyl azide, proceeds through the SN1 mechanism, while the second part of the reaction, namely the formation of the triazole ring, proceeds through an interesting pathway. The probable reason may be that in benzyl halides the positive charge at benzylic position is stabilized due to conjugation with the phenyl ring, on the other hand, sodium azide is a weak nucleophile, therefore, the suggested pathway is SN1. Coordination of Cu(I) to the alkyne is slightly endothermic in MeCN, but exothermic in water, which is in agreement with an observed rate acceleration in water. However, coordination of Cu to the acetylene does not accelerate a 1,3-dipolar cycloaddition. Such a process has been calculated to be even less favorable than the uncatalyzed 1,3-dipolar cycloaddition.

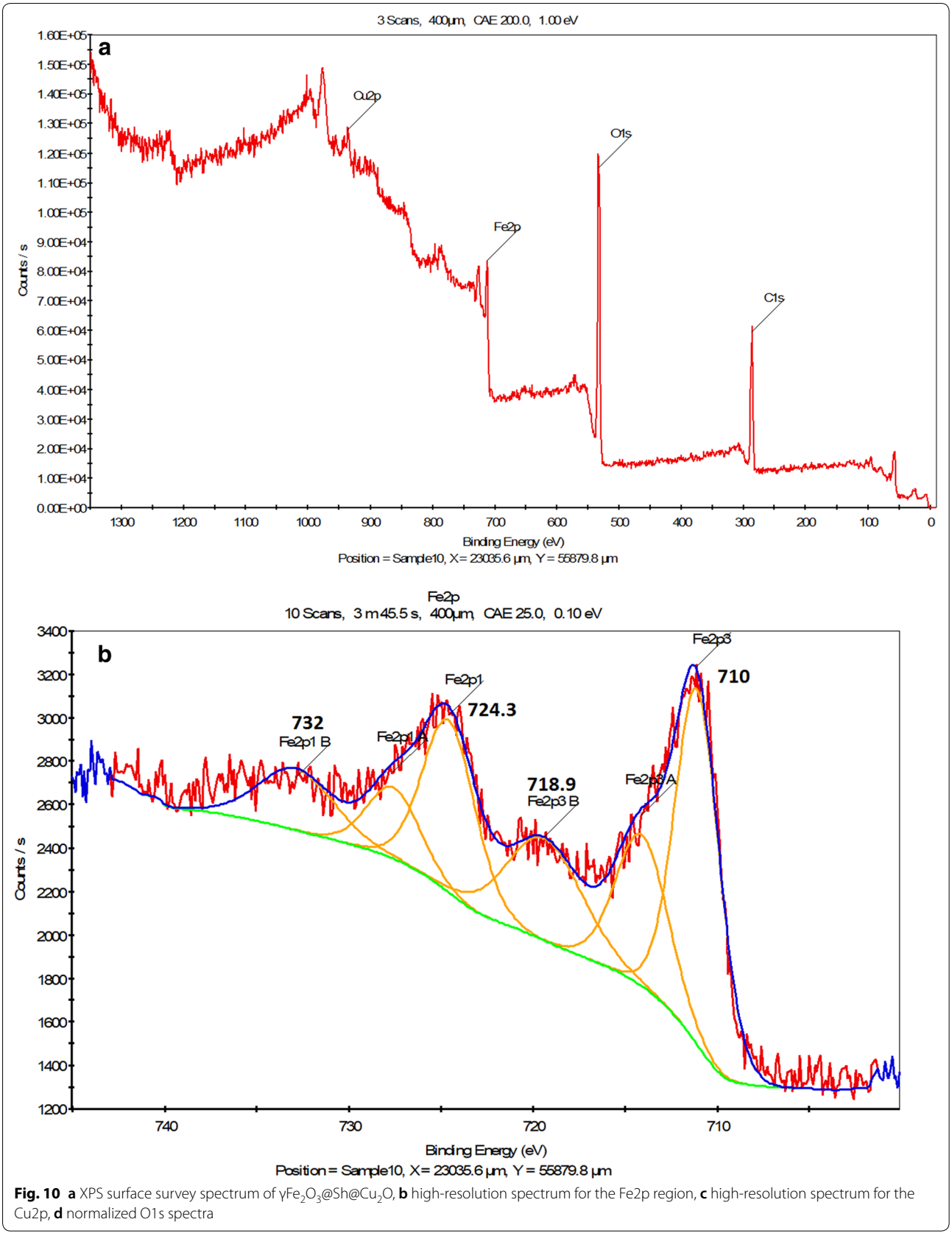

Fig. 10 **a** XPS surface survey spectrum of γFe_2O_3@Sh@Cu_2O, **b** high-resolution spectrum for the Fe2p region, **c** high-resolution spectrum for the Cu2p, **d** normalized O1s spectra

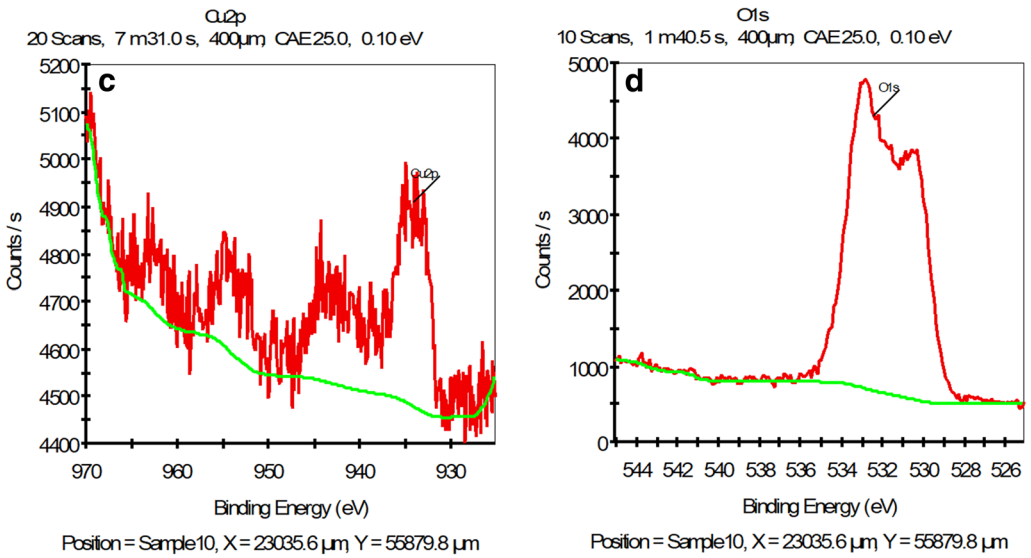

Fig. 10 continued

Instead, an σ-bound copper acetylide bearing a π-bound copper coordinates the azide. Then, an unusual six-membered copper metallacycle is formed. The 2nd copper atom acts as a stabilizing donor ligand. Ring contraction to a triazolyl-copper derivative is followed by protonolysis that delivers the triazole product and closes the catalytic cycle [43] (Fig. 17). The final product of this three-component reaction here is 1,4-diaryl-1,2,3-triazole. These results have successfully demonstrated that this catalyst can easily be used for the synthesis of the click synthesis of 1,4-disubstiuted-1,2,3-triazoles.

To compare the catalytic activity of the synthesized catalyst with other reported heterogeneous catalysts for the three-component reaction of benzyl bromide, sodium azide and phenyl acetylene, the TON and TOF are calculated and tabulated in Table 4. As it can be perceived, γFe_2O_3@Sh@Cu_2O shows higher TON and TOF (entry 7, Table 4).

Conclusion

In summary, a recyclable hybrid magnetic mesoporous material γFe_2O_3@Sh@Cu_2O was developed by click reaction between Sh decorated Fe_3O_4 and copper acetate. The analysis revealed that during coating of Fe_3O_4@Sh using copper salt (II), synchronized redox sorption of Cu^{II} to Cu^{I} occurs at the same time as the oxidation of Fe_3O_4 to γFe_2O_3.

γFe_2O_3 @Sh@Cu_2O exhibited outstanding catalytic activity for regioselective synthesis of 1,4-disubstituated-1,2,3-triazoles via one pot three-component click reaction of sodium azide, terminal alkynes and benzyl halides in the absence of any reducing agent and base. Mild reaction condition, high yields, high TON and TOF, easy separation of the catalyst using an external magnet, efficient recyclability, and Group-Assisted Purification (GAP) avoiding column chromatography or recrystallization are the merits of this catalytic process.

Methods

Materials

All reagents and materials were purchased from commercial sources and used without purification. All of them were analytical grade. ^{1}H, ^{13}C NMR spectra were recorded on a Bruker Avance DPX 300. The chemical shifts (δ) are given in parts per million and referenced to TMS internal standard. IR spectra were recorded in KBr on Shimadzu FT-IR spectrometer and are reported in wave numbers (cm^{-1}). All melting points were measured on a capillary melting point apparatus. All sonication processes were performed using a 400-W probe-type ultrasonic homogenizer from Topsonic Company. Scanning electron microscopy (SEM) was recorded on a VEG//TESCAN 100EM10C-KV, and energy dispersive X-ray spectroscopy (EDX) was recorded on a VEG//TESCAN-XMU. Powder X-ray diffraction (PANalytical X'Pert Pro X-ray diffractometer with the Cu Kα), Fourier transform infrared spectroscopy.

Experimental section

Preparation of Fe_3O_4 magnetic nanoparticles

Magnetic Fe_3O_4 was prepared by precipitation method. A mixed solution of ferrous and ferric ions in the molar ratio 1:2 was prepared by dissolving 2.0 g $FeCl_2{\cdot}4H_2O$ (0.01 mmol) and 5.20 g $FeCl_3{\cdot}6H_2O$ (0.02 mmol) in a round-bottom flask with two openings containing

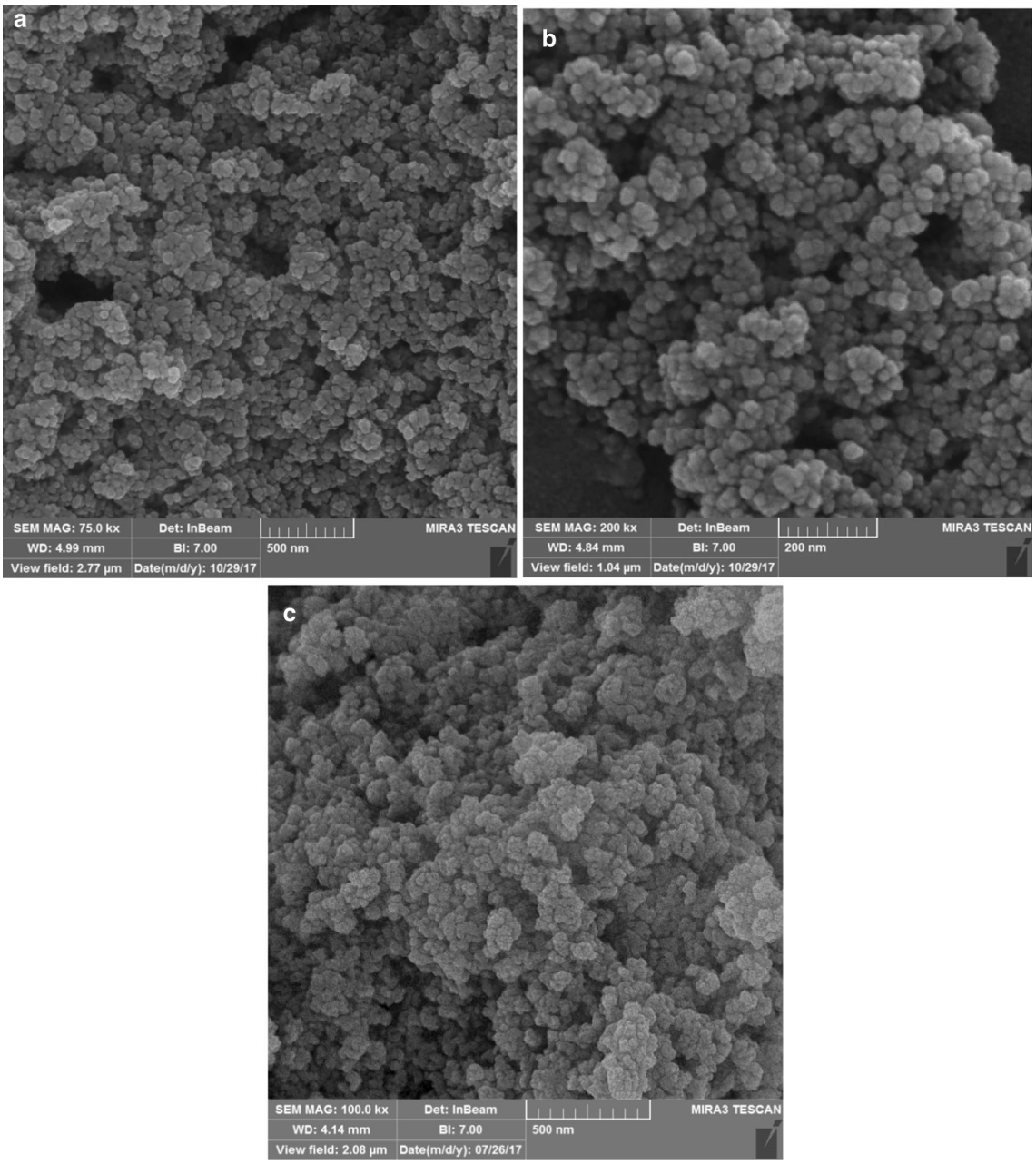

Fig. 11 SEM image of **a** Fe_3O_4, **b** Fe_3O_4@Sh, **c** γFe_2O_3@Sh@Cu_2O

50 mL H_2O. This solution stirrer at room temperature for about 15 min to achieve homogeneity solution, when the homogeneous solution was formed, the temperature was elevated to 70 °C. Under reflux, nitrogen gas and stirring conditions and at 70 °C, the ammonia liquid (about 12 mL) was added dropwise over 1 h until the solution became completely black. The solution was allowed to stirrer under basic conditions for another 45 min. Eventually, the obtained precipitated nanoparticles were separated magnetically, washed with water and EtOH until the pH reached 7, and dried at 60 °C for 2 h.

Surface modification of nano-Fe_3O_4

First, 0.1 g of Sh powder was dispersed in EtOH (10 mL) and sonicated for 1 h at room temperature (solution A). Secondly, a suspension of Fe_3O_4 nanoparticles (0.2 g, 0.86 mmol) in 15 mL EtOH was sonicated for 30 min at room temperature (solution B). Glutaraldehyde (1 mL,

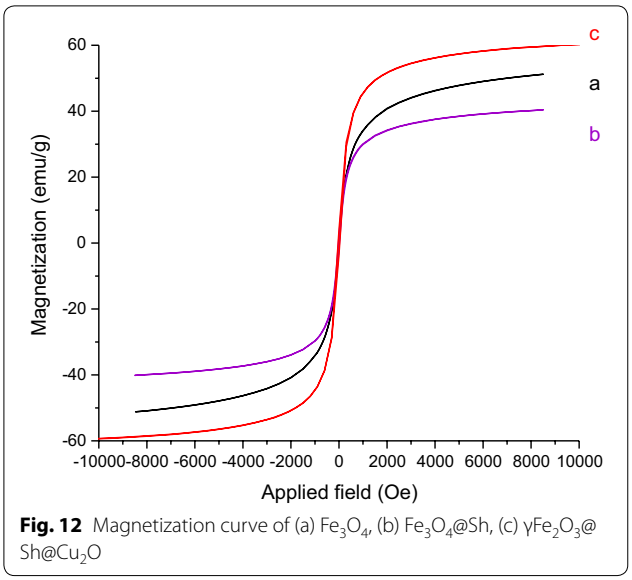

Fig. 12 Magnetization curve of (a) Fe_3O_4, (b) Fe_3O_4@Sh, (c) γFe_2O_3@Sh@Cu_2O

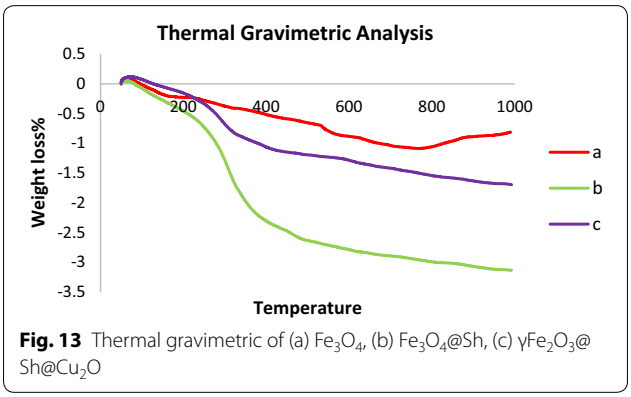

Fig. 13 Thermal gravimetric of (a) Fe_3O_4, (b) Fe_3O_4@Sh, (c) γFe_2O_3@Sh@Cu_2O

Table 1 Optimize the three-component reactions condition of benzyl bromide, sodium azide and phenyl acetylene

Entry	Catalyst (mg)	Solvent	Temperature	Time	Isolated yield %
1	–	–	r.t	48 h	–
2	–	H_2O	r.t	48 h	–
3	–	H_2O	80 °C	48 h	–
4	–	–	80 °C	48 h	–
5	5	H_2O	80 °C	1 h	57
6	5	H_2O:EtOH (1:1)	80 °C	1 h	80
7	5	H_2O:EtOH (1:2)	80 °C	1 h	70
8	5	H_2O:EtOH (2:1)	80 °C	1 h	63
9	5	EtOH	80 °C	1 h	74
10	5	H_2O:EtOH (1:1)	80 °C	45 min	83
11	5	H_2O:EtOH (1:1)	80 °C	2 h	60
12	5	H_2O:EtOH (1:1)	r.t	10 h	80
13	5	H_2O:EtOH (1:1)	100 °C	1:30 h	75
14	10	H_2O:EtOH (1:1)	60 °C	30 min	82
15	20	H_2O:EtOH (1:1)	60 °C	30 min	87
16	30	H_2O:EtOH (1:1)	60 °C	25 min	89
17	40	H_2O:EtOH (1:1)	60 °C	20 min	93
18	50	H_2O:EtOH (1:1)	60 °C	20 min	94

10.6 mmol), as a linker, was then added to the solution B and the mixture was subjected to additional sonication for 30 min at room temperature. Thirdly, solutions A and B are mixed and sonicated for 2 h at room temperature. Finally, the obtained precipitate Fe_3O_4@Sh, was

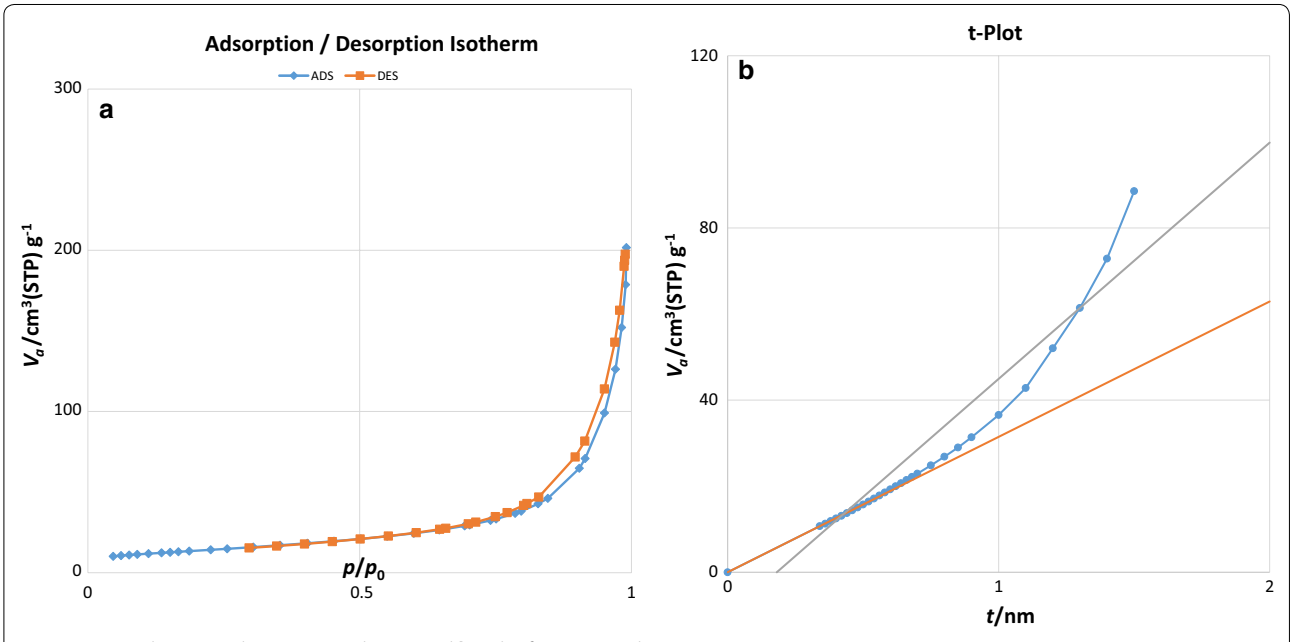

Fig. 14 **a** N_2 adsorption/desorption isotherms and **b** t-plot for γFe_2O_3@Sh@Cu_2O

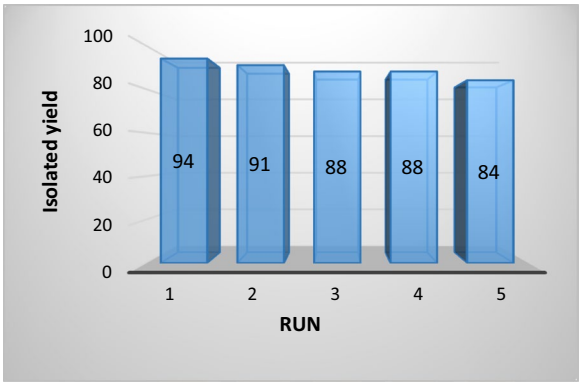

Fig. 15 Reusability of γFe_2O_3@Sh@Cu_2O in the model reaction

Table 2 Screening catalysts for the three-component reaction of benzyl bromide, sodium azide and phenyl acetylene

Entry	Catalyst (30 mg)	Time	Isolated yield
1	Fe_3O_4	5 h	–
2	Sh	5 h	–
3	Fe_3O_4@Sh	5 h	–
4	γFe_2O_3@Sh@Cu_2O	20 min	94
5	HA	5 h	Trace
6	Fe_3O_4@HA	5 h	15
7	Fe_3O_4@HA@Cu	45 min	90
8	$Cu_2Fe_2O_4$, sodium ascorbate	5 h	15
9	$CuBr_2$	5 h	Trace

Experimental conditions: benzyl bromide (1.3 mmol), phenyl acetylene (1.0 mmol), sodium azide (1.3 mmol), catalyst (30 mg), solvent (H_2O:EtOH 2 mL), 60 °C

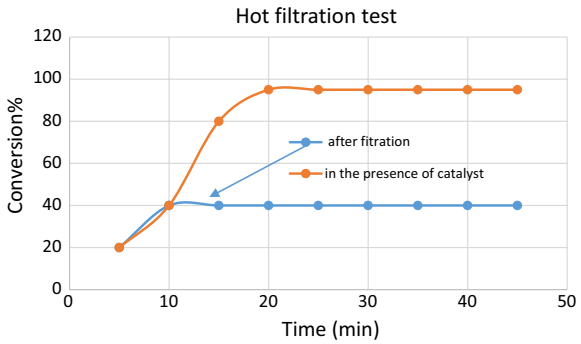

Fig. 16 Hot filtration test to investigate heterogeneous nature of catalyst

magnetically separated, washed several times with EtOH and dried at 60 °C for 12 h.

Immobilization of Cu on Fe_3O_4@Sh

0.4 g of the prepared Fe_3O_4@Sh was magnetically stirred under reflux condition in EtOH (30 mL) until the obtention of a homogeneous solution. A solution of $CuBr_2$ (0.4 g, 0.002 mol) in EtOH (5 mL) was added drop wise to the reaction mixture and mixture stirred for 2 h. Eventually, the catalysts harvested with the aid of a magnet, washed with EtOH Several times and dried at 60 °C for 12 h.

Table 3 Scope of reaction of benzyl halides with alkynes and sodium azide catalyzed by magnetic γFe_2O_3@Sh@Cu_2O

Entry	R^1	R^2	Product	Isolated yield %	Time (min)	TON	TOF (h^{-1})	M.p [refs.]
1	H	H	**4a**	93	20	$3.5*10^5$	$1.0*10^6$	125–127 [9]
2	H	4-Me	**4b**	77	20	$2.9*10^5$	$8.8*10^5$	147–148 [44]
3	H	4-OMe	**4c**	97	25	$3.7*10^5$	$8.9*10^5$	138–140 [20]
4	4-Br	H	**4d**	98	20	$3.7*10^5$	$7.5*10^5$	147–149 [22]
5	4-Br	4-Me	**4e**	72	20	$2.7*10^5$	$8.3*10^5$	165–167 [45]
6	4-Br	4-OMe	**4f**	98	20	$3.7*10^5$	$1.1*10^6$	164–166 [24]
7	4-OMe	H	**4g**	73	20	$2.8*10^5$	$8.4*10^5$	125–127 [46]
8	4-OMe	4-Me	**4h**	57	20	$2.1*10^5$	$8.2*10^5$	132–135 [20]
9	4-OMe	4-OMe	**4i**	66	20	$2.5*10^5$	$7.6*10^5$	98–100 [47]
10	$4\text{-}NO_2$	H	**4j**	53	25	$2.0*10^5$	$6.1*10^5$	152–154 [48]
11	$4\text{-}NO_2$	4-Me	**4k**	50	25	$1.9*10^5$	$5.7*10^5$	242–245 [49]
12	$4\text{-}NO_2$	4-OMe	**4l**	70	25	$2.6*10^5$	$6.4*10^5$	123.5–125.5 [50]
13	2-Cl	H	**4m**	88	20	$3.3*10^5$	$8.1*10^5$	84–86 [9]
14	2-Cl	4-Me	**4n**	88	20	$3.3*10^5$	$8.1*10^5$	117–118 [23]
15	2-Cl	4-OMe	**4o**	75	20	$2.8*10^5$	$3.4*10^5$	137–138[a]

[a] New product

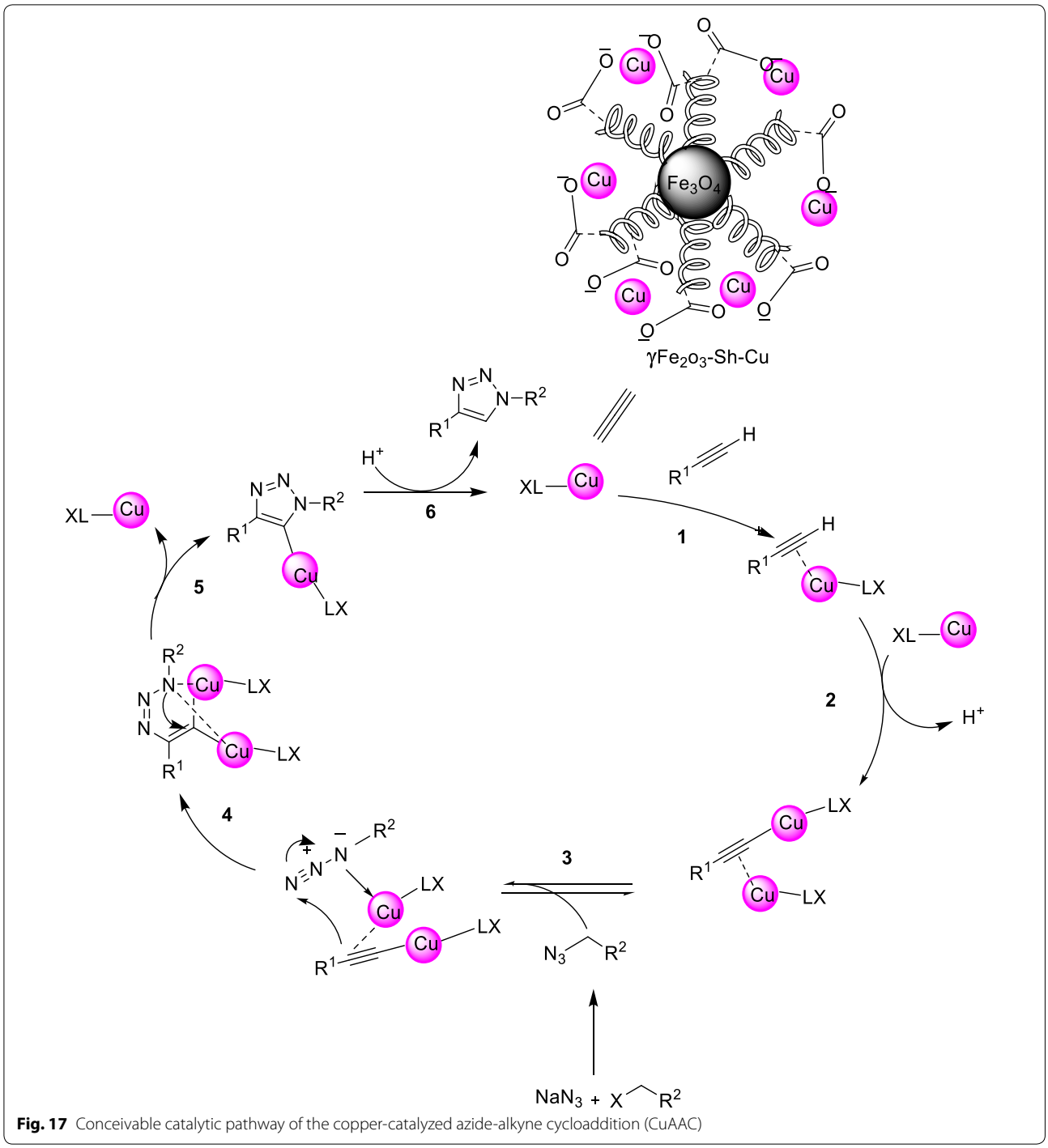

Fig. 17 Conceivable catalytic pathway of the copper-catalyzed azide-alkyne cycloaddition (CuAAC)

General procedure for synthesis of 1,2,3-triazoles in water:EtOH (1:1)

NaN_3 (1.3 mmol), alkyne (1 mmol) and benzyl halide (1.3 mmol) were added to a suspension of γFe_2O_3@Sh@Cu_2O (0.025 mol% Cu, 0.04 g γFe_2O_3@Sh@Cu_2O) in H_2O:EtOH (1:1) (2 mL). The reaction mixture was stirred at 60 °C and monitored by TLC. After completion of the reaction, the catalyst was easily removed from reaction mixture using an external magnet. Then solvent was evaporated with heat and needle-shaped crystals were formed. Finally, crystal products washed with water and normal hexane several times and dried at 60 °C for 6 h.

Table 4 Comparison of three-component reaction of benzyl bromide, sodium azide and phenyl acetylene under different condition using different catalysts

Entry	Catalyst and catalyst loading	Solvent	Condition	Time (min)	Yield (%)	TON	TOF	Refs.
1	$NiFe_2O_4$-glutamate-Cu (1 mol%)	H_2O	r.t	240	92	$9.2*10^3$	$2.3*10^3$	[5]
2	CuNPs@agarose (0.05 mol%)	H_2O	40 °C	480	96	$1.9*10^5$	$2.4*10^4$	[7]
3	OSPs-CuBr[a] (1 mol%)	H_2O	70 °C	240	91	$9.1*10^3$	$2.2*10^3$	[8]
4	Cu/c[b] (5 mol%)	H_2O	100 °C	40	92	$1.8*10^3$	$2.8*10^3$	[9]
5	Cu cat[c] (0.25 mol%) Sodium ascorbate (10 mol%)	t-BuOH: H_2O (1:3)	50 °C	90	99	$3.9*10^4$	$2.6*10^4$	[17]
6	MNPs@FGly[d] (0.5 mol%) Sodium ascorbate	t-BuOH: H2O	60 °C	240	99	$1.9*10^4$	$4.9*10^3$	[19]
7	Cu/SD[e] (6 mol%)	H_2O	Sonication	15	95	$1.6*10^3$	$6.3*10^3$	[51]
8	γFe_2O_3@Sh@Cu_2O (0.025 mol%)	H_2O:EtOH (1:1)	60 °C	20	93	$3.7*10^5$	$1.0*10^6$	This work

[a] Oyster shell powders

[b] Cu(I) on charcoal

[c] Self-assembled polymeric imidazole-copper catalyst

[d] Fe_3O_4-silicacoated@functionalized 3-glycidoxypropyltrimethoxysilane

[e] Copper/sandarac

Leaching test

To determine the copper leakage from the catalyst during the reaction, leaching test was performed hot filtration test for click reaction of benzyl halide **1**, phenylacetylene **3** and Sodium azide. The catalytically active particles were removed from the reaction by filtration after 10 min using a hot frit. After hot filtration, the yield of the reaction no longer changes and stagnates at around 40%.

Characterization data

1-(4-Bromobenzyl)-4-(4-methoxyphenyl)-1,2,3-triazole (**4f**). White solid; IR (KBr): 3087, 3043, 3010, 2956, 2929, 2900, 2831, 1612, 1558, 1492, 1454, 1350, 1298, 1249, 1078, 1029, 821, 761, 524, 476 cm^{-1}. ^1H NMR (DMSO, 300 MHZ) δ = 3.774 (s, 3H), δ = 5.619 (s, 2H), δ = 7.013 (d, J = .028, 2H), δ = 7.320 (d, J = 0.027, 2H), δ = 7.599 (d, J = 0.027, 2H), δ = 7.782 (d, J = .027, 2H), δ = 8.527 (s, 1H) ppm; ^{13}C NMR ($CDCl_3$, 75 MHZ) δ = 52.724, 55.629, 114.781, 121.079, 121.867, 123.718, 127.028, 130.606, 132.162, 135.897, 147.130, 159,546 ppm.

1-(2-Chlorobenzyl)-4-(4-methoxyphenyl)-1*H*-1,2,3-triazole (**4o**). White solid; IR (KBr): 3113, 3107, 2997, 2933, 2835, 1614, 1560, 1498, 1448, 1249, 1174, 1035, 829, 752, 700, 609, 526 cm^{-1}. ^1H NMR (DMSO, 300 MHZ) δ = 3.382 (s, 3H), δ = 3.784 (s, 3H), δ = 5.738 (s, 2H), δ = 6.996 (d, J = 0.02, 2H), δ = 7.283 (t, j = 0.11, 3H), δ = 7.784 (d, J = 0.02, 2H), δ = 8.499 (s, 1H); ^{13}C NMR ($CDCl_3$, 75 MHZ) δ = 51.193, 55.602, 114.752, 121.379, 123.657, 125.411, 127.052, 128.220, 130.089, 130.679, 130.918, 133.085,133.716, 146.921, 159.526 ppm.

1-(2-Chlorobenzyl)-4-(*p*-tolyl)-1*H*-1,2,3-triazole (**4n**). White solid; IR (KBr): 3124, 3060, 2970, 2937, 2777, 1654, 1590, 1443, 1425, 1350, 1288, 1220, 1203, 1100, 1082, 1043, 1016, 860, 838, 802, 781, 730, 690, 538 cm^{-1}. ^{1}HNMR (DMSO, 300 MHZ) δ = 2.313 (s, 3H), δ = 5.743 (s, 2H), δ = 7.228 (m, 3H), δ = 7.351 (m, 2H), δ = 7.5714 (d, J = 0.021, 1H), δ = 7.745 (d, J = 0.026, 2H), δ = 8.557 (s, 1H); ^{13}C NMR ($CDCl_3$, 75 MHZ) δ = 51.221, 121.882, 125.643, 128.200, 128.320, 129.867, 130.086, 130.680, 130.954, 133.117, 133.668, 137.690, 147.054 ppm.

Supplementary information

Supplementary information accompanies this paper at https://doi.org/10.1186/s13065-019-0657-9.

Additional file 1. Figure S1. ^{1}HNMR of 1-(4-bromobenzyl)-4-(4-methoxyphenyl)-1,2,3-triazole. **Figure S2.** Expanded ^{1}HNMR spectra of 1-(4-bromobenzyl)-4-(4-methoxyphenyl)-1,2,3-triazole (aromatic region). **Figure S3.** ^{13}CNMR of 1-(4-bromobenzyl)-4-(4-methoxyphenyl)-1,2,3-triazole. **Figure S4.** ^{13}CNMR of 1-(4-bromobenzyl)-4-(4-methoxyphenyl)-1,2,3-triazole. **Figure S5.** ^{1}HNMR of 1-(2-chlorobenzyl)-4-(4-methoxyphenyl)-1H-1,2,3-triazole. **Figure S6.** Expanded ^{1}HNMR spectra of 1-(2-chlorobenzyl)-4-(4-methoxyphenyl)-1*H*-1,2,3-triazole (aromatic region). **Figure S7.** ^{13}CNMR of 1-(2-chlorobenzyl)-4-(4-methoxyphenyl)-1*H*-1,2,3-triazole. **Figure S8.** Expanded ^{13}CNMR spectra of 1-(2-chlorobenzyl)-4-(4-methoxyphenyl)-1H-1,2,3-triazole. **Figure S9.** ^{1}HNMR of 1-(2-chlorobenzyl)-4-(4-*p*-tolyl)-1*H*-1,2,3-triazole. **Figure S10.** Expanded ^{1}HNMR spectra of 1-(2-chlorobenzyl)-4-(*p*-tolyl)-1*H*-1,2,3-triazole (aromatic region). **Figure S11.** ^{13}CNMR of 1-(2-chlorobenzyl)-4-(*p*-tolyl)-1*H*-1,2,3-triazole. **Figure S12.** Expanded ^{13}CNMR spectra of 1-(2-chlorobenzyl)-4-(p-tolyl)-1*H*-1,2,3-triazole.

Abbreviations

BET: Brunauer–Emmett–Teller; BJH: Barrett–Joyner–Halenda; CuAAC: copper-catalyzed azide-alkyne cycloaddition; EDX: energy-dispersive X-ray spectroscopy; FESEM: field emission scanning electron microscopy; FGly: functionalized 3-glycidoxypropyltrimethoxysilane; FGT: ferrite-glutathione-copper; FTIR:

Fourier transform infrared; HA: humic acid; HMOP: hierarchical mesoporous organic polymer; ICP: inductively coupled plasma; MNPs: magnetic nanoparticles; NPs: nanoparticles; OSPs: oyster shell powders; SBA: Santa Barbara Amorphous; SEM: scanning electron microscopy; Sh: Shilajit; TGA: thermal gravimetric analysis; TON: turnover number; TOF: turnover frequency; vsm: vibrating sample magnetometer; XPS: X-ray photoelectron spectroscopy; XRD: X-ray diffraction.

Acknowledgements
Not applicable.

Authors' contributions
FN and SJ conceived and conducted the experiments and analyzed the results. All authors reviewed the manuscript. Both authors read and approved the final manuscript.

Funding
The authors have no funding to report.

Availability of data and materials
All data generated or analysed during this study are included in this published article and Additional files.

Competing interests
The authors declare that they have no competing interests.

Received: 20 October 2019 Accepted: 18 December 2019
Published online: 07 January 2020

References

1. Rostovtsev VV, Green LG, Fokin VV, Sharpless KB (2002) A stepwise huisgen cycloaddition process: copper(I)-catalyzed regioselective "ligation" of azides and terminal alkynes. Angew Chem Int Ed 41:2596–2599
2. Tornøe CW, Christensen C, Meldal M (2002) Peptidotriazoles on solid phase:[1,2,3]-triazoles by regiospecific copper(I)-catalyzed 1,3-dipolar cycloadditions of terminal alkynes to azides. J Org Chem 67:3057–3064
3. Boningari T et al (2010) Zeo-click chemistry: copper(I)-zeolite-catalyzed cascade reaction; one-pot epoxide ring-opening and cycloaddition. Eur J Org Chem 33:6338–6347
4. Naeimi H, Nejadshafiee V (2014) Efficient one-pot click synthesis of β-hydroxy-1,2,3-triazoles catalyzed by copper(I)@phosphorated SiO_2 via multicomponent reaction in aqueous media. New J Chem 38:5429–5435
5. Lu J et al (2015) One-pot three-component synthesis of 1,2,3-triazoles using magnetic $NiFe_2O_4$-glutamate-Cu as an efficient heterogeneous catalyst in water. RSC Adv 5:59167–59185
6. Girard C et al (2006) Reusable polymer-supported catalyst for the [3 + 2] Huisgen cycloaddition in automation protocols. Org Lett 8:1689–1692
7. Gholinejad M, Jeddi N (2014) Copper nanoparticles supported on agarose as a bioorganic and degradable polymer for multicomponent click synthesis of 1,2,3-triazoles under low copper loading in water. ACS Sustain Chem Eng 2:2658–2665
8. Xiong X, Cai L, Jiang Y, Han Q (2014) Eco-efficient, green, and scalable synthesis of 1,2,3-triazoles catalyzed by Cu(I) catalyst on waste oyster shell powders. ACS Sustain Chem Eng 2:765–771
9. Sharghi H, Khalifeh R, Doroodmand MM (2009) Copper nanoparticles on charcoal for multicomponent catalytic synthesis of 1,2,3-triazole derivatives from benzyl halides or alkyl halides, terminal alkynes and sodium azide in water as a 'Green' solvent. Adv Synth Catal 351:207–218
10. Alonso F, Moglie Y, Radivoy G, Yus M (2010) Multicomponent synthesis of 1,2,3-triazoles in water catalyzed by copper nanoparticles on activated carbon. Adv Synth Catal 352:3208–3214
11. Varma RS (2014) Nano-catalysts with magnetic core: sustainable options for greener synthesis. Sustain Chem Process 2:11
12. Mukherjee N, Ahammed S, Bhadra S, Ranu BC (2013) Solvent-free one-pot synthesis of 1,2,3-triazole derivatives by the 'Click' reaction of alkyl halides or aryl boronic acids, sodium azide and terminal alkynes over a Cu/Al_2O_3 surface under ball-milling. Green Chem 15:389–397
13. Elayadi H et al (2010) Straightforward synthesis of triazoloacyclonucleotide phosphonates as potential HCV inhibitors. Bioorg Med Chem Lett 20:7365–7368
14. Phillips OA, Udo EE, Abdel-Hamid ME, Varghese R (2009) Synthesis and antibacterial activity of novel 5-(4-methyl-1H-1,2,3-triazole) methyl oxazolidinones. Eur J Med Chem 44:3217–3227
15. Lauria A et al (2014) 1,2,3-Triazole in heterocyclic compounds, endowed with biological activity, through 1,3-dipolar cycloadditions. Eur J Org Chem 16:3289–3306
16. Pérez-Balderas F et al (2003) Multivalent nezeoglycoconjugates by regiospecific cycloaddition of alkynes and azides using organic-soluble copper catalysts. Org Lett 5:1951–1954
17. Yamada YM, Sarkar SM, Uozumi Y (2012) Amphiphilic self-assembled polymeric copper catalyst to parts per million levels: click chemistry. J Am Chem Soc 134:9285–9290
18. Fujiki K et al (2017) One-pot three-component double-click method for synthesis of [67 Cu]-labeled biomolecular radiotherapeutics. Sci Rep 7:1912
19. Moghaddam FM, Ayati SE (2015) Copper immobilized onto a triazole functionalized magnetic nanoparticle: a robust magnetically recoverable catalyst for "click" reactions. RSC Adv 5:3894–3902
20. Chavan PV et al (2014) Cellulose supported cuprous iodide nanoparticles (cell-CuI NPs): a new heterogeneous and recyclable catalyst for the one pot synthesis of 1,4-disubstituted-1,2,3-triazoles in water. RSC Adv 4:42137–42146
21. Wang L, Cai C (2010) Reusable polymer-supported copper catalyst for one-pot synthesis of 1-alkyl-and 1-aryl-1,2,3-triazoles: green, simple, and effective. Green Chem Lett Rev 3:121–125
22. Pourjavadi A, Motamedi A, Hosseini SH, Nazari M (2016) Magnetic starch nanocomposite as a green heterogeneous support for immobilization of large amounts of copper ions: heterogeneous catalyst for click synthesis of 1,2,3-triazoles. RSC Adv 6:19128–19135
23. Jia Z, Wang K, Li T, Tan B, Gu Y (2016) Functionalized hypercrosslinked polymers with knitted N-heterocyclic carbene-copper complexes as efficient and recyclable catalysts for organic transformations. Catal Sci Technol 6:4345–4355
24. Sau SC, Roy SR, Sen TK, Mullangi D, Mandal SK (2013) An abnormal N-heterocyclic carbene-copper(I) complex in click chemistry. Adv Synth Catal 355:2982–2991
25. Pérez JM, Crosbie P, Lal S, Díez-González S (2016) Copper(I)–phosphinite complexes in click cycloadditions: three-component reactions and preparation of 5-iodotriazoles. ChemCatChem 8:2222–2226
26. Kaboudin B, Mostafalu R, Yokomatsu T (2013) Fe_3O_4 nanoparticle-supported Cu(II)-β-cyclodextrin complex as a magnetically recoverable and reusable catalyst for the synthesis of symmetrical biaryls and 1,2,3-triazoles from aryl boronic acids. Green Chem 15:2266–2274
27. Roy S, Chatterjee T, Pramanik M, Roy AS, Bhaumik A, Islam SM (2014) Cu(II)-anchored functionalized mesoporous SBA-15: an efficient and recyclable catalyst for the one-pot Click reaction in water. J Mol Catal A Chem 386:78–85
28. Basu P, Bhanja P, Salam N, Dey TK, Bhaumik A, Das D, Islam SM (2017) Silver nanoparticles supported over Al_2O_3@ Fe_2O_3 core-shell nanoparticles as an efficient catalyst for one-pot synthesis of 1,2,3-triazoles and acylation of benzyl alcohol. Mol Catal 439:31–40
29. Samaraj E, Bhaumik A, Manickam S (2019) An efficient Cu^{-} mesoporous organic nanorod for Frieldländer quinoline synthesis, aerobic oxidative dehydrogenation, and click reactions. ChemCatChem. https://doi.org/10.1002/cctc.201900860
30. Hudson R, Feng Y, Varma RS, Moores A (2014) Bare magnetic nanoparticles: sustainable synthesis and applications in catalytic organic transformations. Green Chem 16:4493–4505
31. Zeng T et al (2010) Fe_3O_4 nanoparticle-supported copper (I) pybox catalyst: magnetically recoverable catalyst for enantioselective direct-addition of terminal alkynes to imines. Org Lett 13:442–445
32. Dicks A, Hent A (2014) Green chemistry metrics: a guide to determining and evaluating process greenness. Springer, Cham
33. Agarwal SP et al (2007) Shilajit: a review. Phyther Res 21:401–405
34. Ghosal S (1990) Chemistry of shilajit, an immunomodulatory ayurvedic rasayan. Pure Appl Chem 62:1285–1288
35. Lal VK, Panday KK, Kapoor ML (1988) Literary support to the vegetable origin of shilajit. Anc Sci Life 7:145

36. Khanna R, Witt M, Anwer MK, Agarwal SP, Koch BP (2008) Spectroscopic characterization of fulvic acids extracted from the rock exudate shilajit. Org Geochem 39:1719–1724
37. Grau-Crespo R, Al-Baitai AY, Saadoune I, De Leeuw NH (2010) Vacancy ordering and electronic structure of γ-Fe_2O_3 (maghemite): a theoretical investigation. J Phys Condens Matter 22:255401
38. Asgari S, Fakhari Z, Berijani S (2014) Synthesis and characterization of Fe_3O_4 magnetic nanoparticles coated with carboxymethyl chitosan grafted sodium methacrylate. J Nanostruct 4:55–63
39. Zhang YX, Huang M, Li F, Wen ZQ (2013) Controlled synthesis of hierarchical CuO nanostructures for electrochemical capacitor electrodes. Int J Electrochem Sci 8:8645–8661
40. Cao D et al (2016) High saturation magnetization of γ-Fe_2O_3 nanoparticles by a facile one-step synthesis approach. Sci Rep 6:32360
41. Rao PM, Zheng X (2011) Unique magnetic properties of single crystal γ-Fe_2O_3 nanowires synthesized by flame vapor deposition. Nano Lett 11:2390–2395
42. Storck S, Bretinger H, Maier WF (1998) Characterization of micro-and mesoporous solids by physisorption methods and pore-size analysis. Appl Catal A 174:137–146
43. Worrell BT, Malik JA, Fokin VV (2013) Direct evidence of a dinuclear copper intermediate in Cu(I)-catalyzed azide-alkyne cycloadditions. Science 340:457–460
44. Sun S, Bai R, Gu Y (2014) From waste biomass to solid support: lignosulfonate as a cost-effective and renewable supporting material for catalysis. Chem Eur J 20:549–558
45. Mishra A et al (2017) A peerless aproach: organophotoredox/Cu(I) catalyzed, regioselective, visible light facilitated, click synthesis of 1,2,3-triazoles via azide-alkyne [3 + 2] cycloaddition. Catal Lett 147:2600–2611
46. Gupta M, Paul S, Kant R, Gupta VK (2015) One-pot synthesis of 1,4-disubstituted 1,2,3-triazoles via Huisgen 1,3-dipolar cycloaddition catalysed by SiO_2–Cu(I) oxide and single crystal X-ray analysis of 1-benzyl-4-phenyl-1*H*-1,2,3-triazole. Monatshefte für Chemie-Chemical Mon 146:143–148
47. Linares D, Bottzeck O, Pereira O, Praud-Tabariès A, Blache Y (2011) Designing 2-aminoimidazole alkaloids analogs with anti-biofilm activities: structure-activities relationships of polysubstituted triazoles. Bioorg Med Chem Lett 21:6751–6755
48. Meng X, Xu X, Gao T, Chen B (2010) Zn/C-catalyzed cycloaddition of azides and aryl alkynes. Eur J Org Chem 28:5409–5414
49. Naeimi H, Shaabani R (2017) Ultrasound promoted facile one pot synthesis of triazole derivatives catalyzed by functionalized graphene oxide Cu(I) complex under mild conditions. Ultrason Sonochem 34:246–254
50. Reddy V, Reddy YV, Sridhar B, Reddy BV (2016) Green catalytic process for click synthesis promoted by copper oxide nanocomposite supported on graphene oxide. Adv Synth Catal 358:1088–1092
51. Faeghi F, Javanshir Sh, Molaei Sh (2018) Natural polymer-based copper/sandarac resin catalyzed regioselective one-pot synthesis of 1,4-disubstituted 1,2,3-triazoles under ultrasonic. ChemistrySelect 3:11427–11434

Publisher's Note